

Preparation of YSZ electrolytes for solid oxide fuel cells (SOFC) by electrostatic spray deposition

S. Uhlenbruck*, T. Hoppe, H.P. Buchkremer and D. Stöver

Forschungszentrum Jülich GmbH, Institute for Materials and Processes in Energy Systems, IWW, D-52425 Jülich, Germany

Yttrium- and zirconium-containing solutions, so-called precursors, were deposited by electrostatic spray deposition on anode substrates of solid oxide fuel cells. Metal-organic precursors as well as nitrate-based precursors were used. The influence of the deposition temperature, the ion concentration in the solution, the type of solvent, the spray distance and the high voltage on the layer morphology is discussed. Leakage rate measurements were carried out to qualify the gas-tightness of the layers produced.

Key words: Fuel cells, ZrO_2 , Precursors-organic, Electrostatic spray deposition

Introduction

Fuel cells are “direct” converters of chemical energy into electrical energy, without the intermediate steps of generating heat and mechanical energy as necessary in conventional heat engines. There are many types of fuel cells, which mainly differ in their temperature of operation. Among them, ceramic high-temperature fuel cells or solid oxide fuel cells (SOFCs) operate at the highest temperatures, around 800-1000 °C. These temperatures are high enough to convert oxygen and hydrogen into water and energy without any special catalyst, in contrast to low temperature fuel cells which need platinum catalysts for this electrochemical reaction. Moreover, carbon monoxide (CO) is converted to carbon dioxide (CO_2) and desorbed from the hot surface of the SOFC electrodes. Thus, carbon monoxide is not a poison for the SOFC. This is especially advantageous when using, for example, methane instead of hydrogen as a fuel: due to the catalytic activity of the SOFC anode methane is reformed to CO (or to CO_2 in the case of a water gas shift reaction or an electrochemical oxidation) and hydrogen.

The SOFC consists of two porous electrodes and a ceramic electrolyte that separates the fuel gas chamber and the oxygen (or air) chamber. A dense electrolyte is required in order to prevent a gas exchange between these two chambers. Yttria-stabilized zirconia (YSZ) is currently widely used as the electrolyte material because of its chemical stability, its considerable conductivity for oxygen ions and its high electronic resistance. The electrolyte is commonly applied in the form of fine

powders (having sub- micrometre particle sizes) and organic additives, by means of slurry coating, screen printing or powder spraying and subsequent sintering. A major drawback is the high sintering temperature of 1300-1400 °C necessary for this particle size, and – as a rule of thumb – a minimum of around 5 to 10 layers of particles to obtain gas-tight layers; this means that there is a lower limit of electrolyte thickness of about two to five micrometres.

One possible approach is to apply yttrium- and zirconium-containing solutions (e.g. metal-organic compounds), so-called precursors, which are pyrolyzed on the surface of one electrode to build a dense YSZ layer.

In this paper, the application of YSZ layers on anode substrates of SOFC with dimensions of 20 mm×20 mm using several precursors is described. These precursors are processed by a spray technique that uses the repulsive forces of equal charges to create a spray from the precursor liquid (‘electrostatic spray deposition (ESD)’) [1-5].

Experimental Procedure

Preparation of precursors

Two different types of precursors were used: (i) zirconium acetyl acetonate (Merck, Germany) and yttrium acetyl acetonate (Alfa Aesar Johnson Matthey, Germany); (ii) zirconium oxynitrate hydrate and yttrium nitrate hydrate (Fluka Chemie, Germany). In each series of experiments the zirconium and yttrium precursors were mixed in such a way that the mixture contained 16 mol% of yttrium and 84 mol% of zirconium (corresponding to 8 mol% Y_2O_3 fully stabilized ZrO_2 , [YSZ]).

Experiments with the first set of precursor salts (i) were based on experiments carried out by Chen and

*Corresponding author:
Tel : +49-2461-61-5984
Fax: +49-2461-61-2455
E-mail: s.uhlenbruck@fz-juelich.de

Schoonman [1]. Ethanol, butyl carbitol [or: diethylene glycol monobutyl ether] (Aldrich, Germany), terpineol, glycerin and water were tested as solvents. The solvents were varied in order to obtain solutions which differed in specific heat, in surface tension, viscosity, solvent boiling point and electrical conductivity – parameters that directly influence the spraying and the pyrolysis of the precursors.

For the second set of precursors water was used as the solvent.

ESD device

A sketch of the commercial ESD device (AST Advanced Surface Technology, The Netherlands) used is shown in Fig. 1. The precursor is contained in a syringe in a syringe pump and is pumped to the capillary (stainless steel, diameter: 0.9 mm, apex angle: 23°). An electric field (potential difference 0–35 kV) between the capillary and the substrate holder generates a spray from the liquid drops at the tip of the capillary as follows. The drop at the tip of the capillary is charged by the electrical potential. The amount of charge Q depends on the potential $U_{el.}$ and the radius R of the drop:

$$U_{el.} = -\frac{Q^2}{4\pi\epsilon_0 R},$$

where ϵ_0 is the dielectric constant. The resulting repulsive Coulomb forces of even charges act against the attractive forces due to the surface tension σ of the liquid (potential energy: $U_\sigma = 4\pi R^2 \sigma$).

The drop is regarded as stable as long as the attractive surface tension forces are greater than the repulsive forces of the accumulated charges. If the Coulomb forces are greater than the surface tension forces the drop becomes unstable. It can be shown mathematically that the stable region can be reached by a change from one large drop to several smaller drops due to the different radius dependence of $U_{el.}$ and U_σ (spray generation). Thus a spraying cone consisting of small charged droplets accelerating to the grounded substrate holder is generated by the applied electrical field.

The substrate to be deposited is mounted on the substrate holder, which can be heated to temperatures of about 700 °C. A thermocouple in the substrate holder near the sample measures the temperature. Although the real deposition temperature depends on the balance of the thermal contact between sample and substrate holder, the sample's thermal conductivity and heat radiation, nevertheless the temperature measured by this thermocouple is hereafter denoted as the deposition temperature.

Prior to the deposition experiments described in the following, the geometrical arrangement of the capillary and substrate holder was tested with regard to spray cone homogeneity. It was found that – depending on the distance between the capillary and the substrate holder and the applied voltage – the spraying cone differed from the assumed circular deposition area on top of the substrate holder towards an ellipsoidal (“two circles”) or to an ensemble of three separate overlapping circles. These deviations can have a direct impact on the homogeneity of the deposited layers.

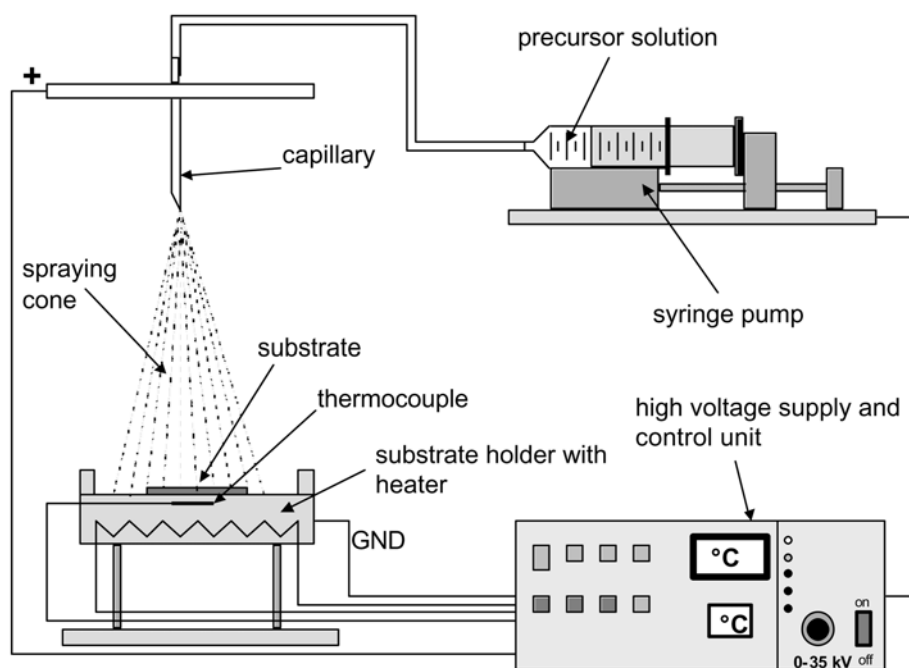


Fig. 1. Scheme of the experimental setup with substrate, substrate holder, metallic capillary and high voltage source (“+” denotes high potential, “GND” is ground). The syringe pump is insulated from the high voltage.

All the experiments described in this article were carried out in “process down mode”, i.e. the capillary was mounted above the substrate and substrate holder.

Two types of substrates were used in these experiments. All of them had dimensions of 20 mm×20 mm×1.5 mm. The first set consisted of a mixture of the ceramic materials NiO and YSZ, sintered at 1400 °C. The second set were prepared in the same way as the first set, except that an additional layer of NiO/YSZ was applied to smooth the top surface (for details of processing see e.g. D. Stöver et al. [6] and references therein). All samples exhibited open porosity.

Image analysis

A quantitative characterization of the electrolyte layer was carried out with the digital image analysis software AnalySIS®. For this analysis, sections of the images with dimensions of 100 µm×100 µm were taken into account. The images were obtained by an optical microscope, Olympus PMG 3, together with a digital camera from Jenoptik, Germany.

Prior to analysis all samples were annealed at 700 °C for one hour to remove all organic or nitrate residues. Polished cross sections of the samples were obtained by embedding the sample in epoxy resin, grinding with SiC grinding paper and polishing with diamond suspension down to 1 µm roughness.

For leakage tests, samples coated with an electrolyte layer were mounted on a cylinder with a hole in such a way that this hole was sealed with the electrolyte layer. The cylinder (with a defined volume) was evacuated by a turbomolecular pump. A valve to the pump was subsequently closed, and the pressure increase inside the cylinder was measured as a function of time.

Results and Discussion

Metal-organic precursors

In Table 1 the results of the solubility tests of precursor set (i) for different solvents are summarized (mixtures of solvents are not considered here).

In general, the solubility of the salts in the solvents under investigation is low compared to many inorganic

Table 1. Solubilities of metal-organic precursors in different solvents.

solvent	solubility in g/l solvent at room temperature (24 °C)	
	zirconium acetyl acetate	yttrium acetyl acetate
ethanol	37.8	1.6
butyl carbitol	2.4	1.0
terpineol	1.3	0.6
glycerine	0.2	0.2
water (deionized)	15.0	almost insoluble

salts (see for example the solubility of the corresponding nitrate salts in the next section).

Among the tested solvents, ethanol showed the highest solubility for zirconium acetyl acetate as well as for yttrium acetyl acetate, followed by butyl carbitol. Since a deposition rate of higher than 1 µm YSZ per hour was desired and flow rates of the solution between about 1 and 10 ml/h were applicable, a minimum precursor concentration in the solutions of more than around 2 g/l (flow rate 10 ml/h) to 20 g/l (flow rate 1 ml/h) solvent was required. Therefore it was decided to abandon any experiments using solvents other than ethanol/butyl carbitol.

Water would have been a candidate for further sets of experiments, since the solubility of zirconium acetyl acetate was high. However, the solubility of yttrium acetyl acetate was too low to obtain an acceptable precursor concentration in such a solution to deposit YSZ with the required molar ratio of 16 mol% Y : 84 mol% Zr.

Variation of deposition temperature

In Fig. 2 and Fig. 3 the influence of deposition temperature on the layer morphology can be seen. At low deposition temperatures a “floe structure” of flat, smooth and dense particles with an extension of about 30 µm, and broad cracks between them was established. The distance between the floes as well as the extension of each floe can be significantly reduced by increasing of the substrate temperature during deposi-

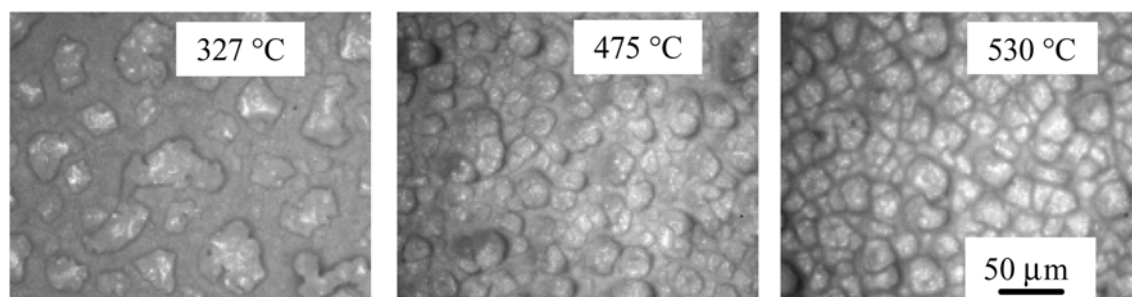


Fig. 2. Optical micrographs of layers deposited at various temperatures (all samples annealed at 700 °C after ESD to remove the organic residues). Parameters: distance capillary-sample: 3 cm; high voltage: 12 kV, flow rate: 6 ml/h; deposition time: 36 minutes; precursor concentration 0.0163 mol/l, solvent: ethanol/butyl carbitol (ratio 1:1).

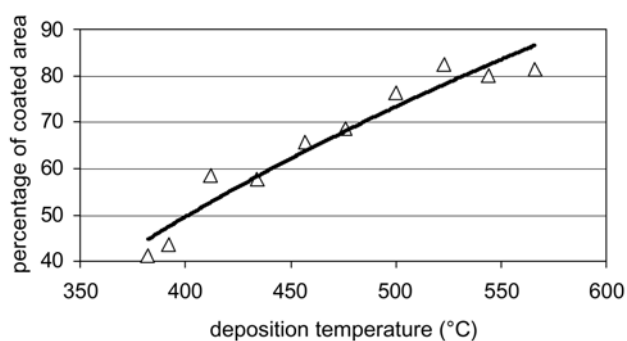


Fig. 3. Percentage of coated sample surface area, determined by image analysis, as a function of the deposition temperature. Triangles denote single data points, the line is a guide for the eyes. The deposition parameters for this series of experiments were the same as in Figure 2.

tion.

These changes in morphology are presumably due to different amounts of organic residues in the layer during deposition. At low deposition temperatures some of the organic ingredients are also deposited. Therefore, the fraction of yttrium and zirconium species in the deposited layer is comparatively low. At high deposition temperatures most of the organic constituents already evaporate or pyrolyze in the spray cone so that the fraction of yttrium and zirconium in the deposited layer is higher. The relative amount of solid material in the layers inevitably influences the sintering of the particles.

Higher deposition temperatures than about 600 °C were not possible because of the increasing thermal radiation of the substrate holder which also heated the adjacent elements. This heating caused a boiling of the ethanol of the precursor solution in the capillary so that the spray cone became unstable.

In another set of experiments the concentration of the precursor in the solution was varied from 0.0163 mol/l to 0.039 mol/l to 0.08 mol/l to 0.16 mol/l. In order to obtain similar thicknesses of the deposited layers the deposition time was reduced in proportion to the concentration of the precursor. Within this range of precursor concentrations neither a trend towards a change in the percentage of coated surface area nor any significant changes in morphology could be identified.

A change in the ethanol/butyl carbitol composition in the solvent with ratios of 50:50, 67:33, 75:25, 80:20 did not result in any significant improvement of the layer morphology.

Influence of spraying distance/high voltage: “hidden parameters”

For the deposition as a function of the distance between the capillary tip and the substrate the parameters were: deposition temperature 425 °C, flow rate 6 ml/h, precursor concentration 0.0163 mol/l and ethanol/ butyl carbitol as a solvent (ratio 1:1). The distance was varied between 1.5 cm and 4.5 cm. It was assumed that

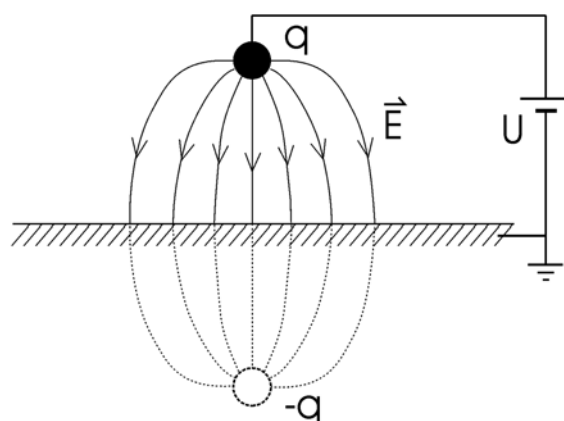


Fig. 4. Sketch of the electrical field between the capillary tip and the substrate holder of the ESD device. The tip charge is denoted q , while U and E are the voltage and the electrical field, respectively.

the apex angle of the spray cone did not change so that the basal area of the spray cone on the substrate changed in proportion to the square of the spraying distance. Since the flow rate remained constant it was also necessary to change the deposition time with the square of the spraying distance, to guarantee a similar layer thickness for all samples.

Changing the distance did not lead to any significant change of the layer morphology or of the percentage of coated surface area of the samples.

At first sight, in this series of experiments apparently only one parameter, the spraying distance, was changed. Actually, several “associated” parameters were changed with the spraying distance, too. This will now be explained by means of Fig. 4.

The tip of the capillary is sketched as a filled sphere in contact with the voltage U . The substrate holder (with the sample) is assumed to be an electron-conducting, earthed plane with an extension that is large compared to the distance d to the tip. In this case, the principle of mirror-image charge can be applied [7]. This principle says that the electrical field of a particle with charge q near a conducting plane is equal to an electrical field of a charged particle q and a mirror-image charge $-q$ placed at a distance of $2d$.

According to Coulomb’s law, the “electrical force” F between the charge q and the mirror-image charge $-q$ (which is then identical to the force between the charge q and the grounded metal plate) is $F = (1/4\pi\epsilon_0) (q^2/4d^2)$, where ϵ_0 is the electrical field constant. Thus, the force varies with the square of the distance d in the case of an insulated charge q (i.e. without electrical connection to the voltage U). Therefore, the electrical field E between the charge q and the metal plate (which is a measure of the electrical forces) is reduced with increasing distance d , so that the acceleration forces for any charged droplets in the electrical field would decrease. On the other hand, since work against the attractive force between the charge and the metal plate

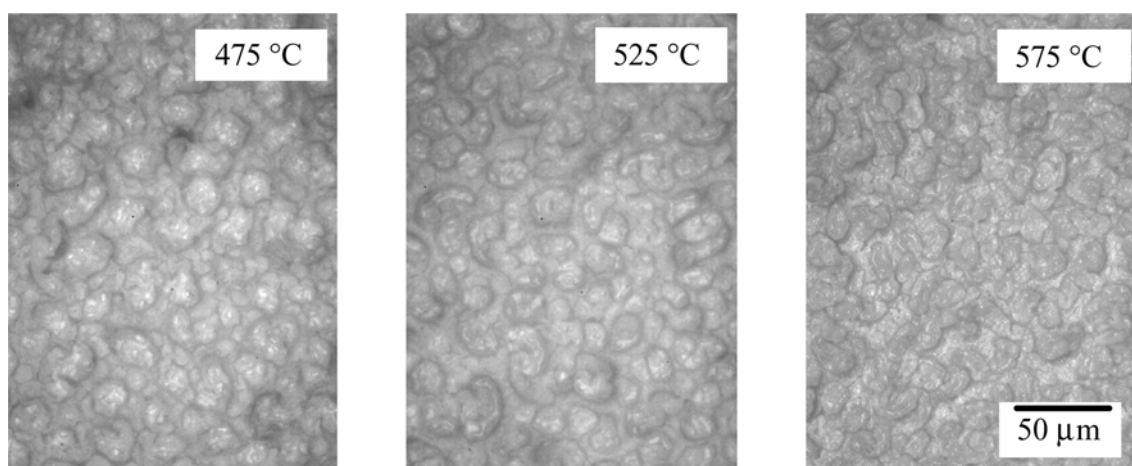


Fig. 5. Optical images of the YSZ electrolyte layers fabricated by multiple deposition and subsequent heat treatment of 700 °C for one hour.

has to be done to increase the distance d , this increases the potential energy and thus the potential difference U between the charge and the metal plate.

Now the case of a charge q that is electrically connected to an external voltage U is discussed.

When the distance d is increased the electrical field at a given point between the charge and the metal plate will also decrease, as discussed in the previous section. However, in this case the potential difference between the charge and the metal plate remains constant: a charged droplet transferred from the tip to the plate would gain the same amount of (potential/kinetic) energy irrespective of the distance d , but at a reduced acceleration rate. Moreover, a constant potential difference means a depletion of charges from the tip during the increase of the distance (the tip-metal plate ensemble can be regarded as a capacitor whose capacity C would decrease with increasing distance d ; therefore, according to $q=C \cdot U$, this implies a reduction of q). A reduced amount of charge on the tip will probably influence the charging behavior of the droplets coming out of the capillary.

Apparently, the percentage of coated surface area seemed to increase with increasing high voltage. Nevertheless, it has to be stressed that in this series of experiments again several “associated” parameters were changed with the voltage. From the previous section it can be concluded that an increase of voltage increases the charge of the capillary tip and thus the electrical field. The droplets will then experience a higher acceleration and will reach the sample surface in a shorter time. However, the change of voltage also affects the shape (i.e. the apex angle) as well as the process stability of the spray cone.

For these reasons, the results of the experiments with distance and voltage variation are not discussed further.

Multiple deposition

The experiments described in the previous sections were carried out in one single, continuous deposition

run. In this section, the effects of three deposition cycles for each sample are discussed. The duration of each cycle was 12 minutes, followed by a break of 15 minutes where the samples remained on the heated substrate holder. The reason for these cycles was to remove a greater amount of the organic species during deposition.

The precursor concentration was 0.0163 mol/l, the spray distance 3 cm, the flow rate 6 ml/h and the high voltage 12.25 kV.

In Fig. 5, the results of the multiple deposition are shown for various deposition temperatures: all samples exhibit a rugged but almost dense surface electrolyte layer. The ruggedness is reduced with increased deposition temperature.

Therefore, leakage rates were determined at samples coated at deposition temperatures between 500–600 °C. Since the surface adhesion of the electrolyte layers annealed at 700 °C was not mechanically stable enough for the leakage tests the samples were sintered at 1100 °C. The layer morphology was found to be mainly unchanged by the additional heat treatment.

The leak rates of the measured samples were in the range of (6 ± 1) mbar·l/s·cm², which is some powers of ten greater than for electrolytes processed by different techniques [8]. Single, comparatively large defects such as open pores or cracks are considered to be the main cause of the high leak rates.

Nitrate-based precursors

The solubility of zirconium oxynitrate hydrate in water was found to be 280 g/l H₂O, while more than 1500 g of yttrium nitrate hydrate could be dissolved per litre of water. The solubility of the nitrate salts in water was considerably higher than the solubility of the metal-organic precursors of the preceding section.

Variation of deposition temperature

The first ESD experiments with this kind of precursor failed due to the high surface tension of the

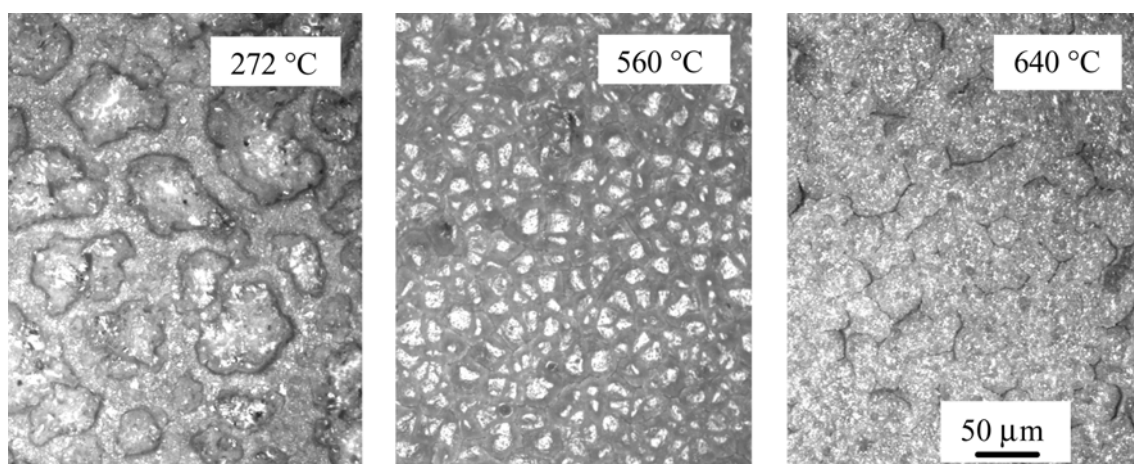


Fig. 6. Optical micrographs of layers coated with nitrate-based precursors at various deposition temperatures (all samples annealed at 700 °C after ESD for removal of organic residues).

liquid which prevented a proper generation of the spray cone. In order to reduce the surface tension tensides and ethanol, respectively, were added. The addition of tensides was detrimental because of flocculation and precipitation of the precursor. With a mixture of 70 wt% of water and 30 wt% of ethanol as a solvent it was possible to create a stable spray cone. Due to a considerably higher ion concentration in the solution (0.32 mol/l) a reduced flow rate of 2.5 ml/h and a deposition time of six minutes were chosen. The spraying distance was 4 cm. It was necessary to increase the high voltage to 15.75 kV because of the changed solvent and the higher ion concentration compared to the metal-organic precursor.

In Fig. 6, optical images of the layers deposited with the nitrate-based precursor after heat treatment at 700 °C are shown. As in the experiments with the metal-organic precursor, the percentage of coated surface area increased with increased deposition temperature (see also Fig. 7). However, for each temperature the percentage of coated surface area with this type of precursor was higher compared to the samples coated with the metal-organic precursor.

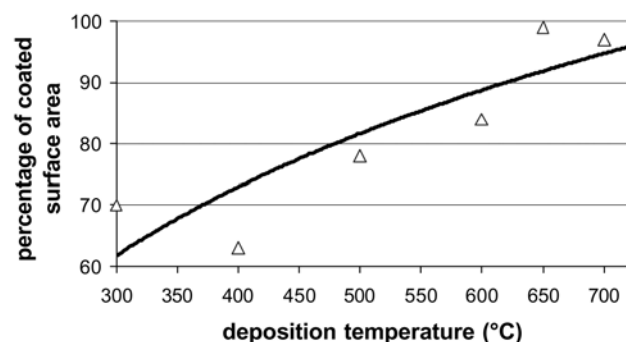


Fig. 7. Percentage of coated surface area, determined by image analysis, as a function of deposition temperature, for samples with nitrate-precursor based layers. Triangles denote single data points, the line is a guide for the eyes. Higher deposition temperatures than 700 °C were not possible with this device.

In another set of experiments, the concentration of the precursor was increased from 0.32 mol/l to 0.64 mol/l. The experiments described in the previous section were repeated with this precursor solution. In the case of nitrate-based precursors this concentration increase lead to apparently significantly denser layers, in contrast to the experiments with metal-organic precursors.

Nevertheless, single, very fine cracks were visible in all samples. These cracks could not be closed by annealing to temperatures of up to 1200 °C for 5 hours. The presence of cracks was also verified by leakage measurements. The leak rate was around 7 mbar·l/s·cm² for all samples.

Conclusions

Metal-organic and nitrate-based precursors were used for electrostatic spray deposition of electrolyte layers.

For the metal-organic precursors, ethanol and butyl carbitol were the solvents with the highest solubility.

The deposited layers exhibited a “floe structure”, where the floes were separated by cracks. With increasing deposition temperature the percentage of coated surface area significantly increased; the floes became smaller, but the distance between them shrank considerably. Apparently, neither a change of precursor concentration, nor of the solvent composition, nor the spray distance nor the accelerating high voltage affected the general layer morphology.

In another set of experiments, multiple deposition runs with intermediate breaks of a few minutes were carried out. This significantly improved the layer morphology with regard to the percentage of coated surface area.

For zirconium oxynitrate and yttrium nitrate water was used as the solvent; the solubility was considerably higher than for all tested combinations of solvents for the metal-organic precursors.

For the nitrate-based precursors the percentage of coated surface area also increased with the deposition temperature. For each temperature the percentage of coated surface area with this type of precursor was higher compared to the samples coated with the metal-organic precursor.

The gas-tightness was tested for all samples whose electrolyte layer was found to be apparently dense. However, the leakage rates were some orders of magnitude higher than those of electrolytes processed by different techniques. This can probably be explained by single defects like cracks or open pores still being present in the layers.

Acknowledgements

The authors thank J. Schoonman, Delft University of Technology, Department of Inorganic Chemistry, The Netherlands, for valuable discussions on electrostatic spray deposition and B. Meester from advanced Surface Technology (AST), 2665 JA Bleiswijk, The Netherlands, for his kind technical support. Partial financial support from the European Science Foundation within the framework of the OSSEP program, no. MCG/OSSEP/2002-19/bol0235, is gratefully acknowledged.

References

1. C. Chen, and J. Schoonman, in "Oxygen Ion and Mixed Conductors and Their Technological Applications", edited by H. L. Tuller, J. Schoonman, and I. Riess (Kluwer Academic Publishers, 2000) p. 295.
2. B. Su and K.L. Choy, *J. Mater. Chem.* 9 (1999) 1629-1633.
3. D. Perednis and L.J. Gauckler, *Solid State Ionics* 166[3] (2004) 229-239.
4. D. Perednis, O. Wilhelm, S.E. Pratsinis, and L.J. Gauckler, *Thin Film Solids*, 474[1] (2005) 84-95.
5. H. Nomura, S. Parekh, J.R. Selman, and S. Al-Hallaj, *J. Appl. Electrochem.* 35[1] (2005) 61-67.
6. D. Stöver, H.P. Buchkremer, and S. Uhlenbruck, *J. Ceram. Int.* 30 (2004) 1107-1113.
7. J.D. Jackson, in "Classical Electrodynamics", (2nd ed., John Wiley & Sons, Inc., New York, Chichester, Brisbane, Toronto, Singapore, 1975) p. 54.
8. R. Förthmann, G. Blaß, and H.P. Buchkremer, in *Proceedings of the Fifth International Symposium on Solid Oxide Fuel Cells (SOFC-V)*, Aachen, Germany, 2-5 June 1997, edited by U. Stimming, S.C. Singhal, H. Tagawa, W. Lehnert (The Electrochemical Society, Pennington, NJ) p.1003.